Progress Report 2009 and Beam Request for 2010

Muon Capture on the Deuteron

The MuSun Experiment

PSI Experiment R-08-01, spokespersons P. Kammel, C. Petitjean, A.A. Vasilyev

MuSun Collaboration [1]

**Petersburg Nuclear Physics Institute –
University of Illinois at Urbana-Champaign – Paul Scherrer Institut –
University of Kentucky – Boston University – Regis University –
University of South Carolina– Université Catholique de Louvain**

http://www.npl.uiuc.edu/exp/musun

Figure 1: First assembly and test of cryo-TPC at PSI, November 2009

Contents

1 Overview

1.1 Physics Update and Experimental Strategy

The goal of the MuSun experiment is a measurement of the rate Λ_d for the semileptonic weak process

$$\mu^- + d \rightarrow \nu_\mu + n + n \tag{1}$$

to a precision of better than 1.5%. Λ_d denotes the capture rate from the doublet hyperfine state of the muonic deuterium atom in its $1s$ ground state.

Muon capture on the deuteron is the simplest weak interaction process on a nucleus and can both be calculated and measured to a high degree of precision. The basic pseudoscalar coupling g_P required for such calculations has been recently measured by the MuCap experiment [2] and will be more precisely determined by its ongoing final analysis. At the same time, effective field theories (EFTs) have been developed to calculate electro-weak observables in few-body systems, following Weinberg's pioneering work [3]. For the case of $\mu + d$ capture, hybrid EFT [4] and pionless EFT [5] have been applied, and a fully self-consistent calculation in a rigorous QCD-based EFT scheme is in preparation by several theory groups [6]. While reaction (1) could serve as the benchmark for the axial current interaction in the two-nucleon system, the experimental situation at present is inadequate to provide much guidance. The best existing experiments [7, 8] are not precise enough and the most precise result differs from modern theory by 3 standard deviations. If true, such a discrepancy would have major ramifications on important astrophysics processes, which are discussed below. The MuSun measurement, based on novel techniques, should exceed the precision of previous efforts by nearly an order of magnitude. The result will provide data of precision commensurate with the anticipated theoretical calculations.

Reaction (1) is closely related to fundamental reactions of astrophysical interest. These include the $p + p$ fusion reaction, which is the primary energy source in the sun and the main sequence stars, and the $\nu + d$ reaction, which provided convincing evidence for solar neutrino oscillation, as both its charged current and neutral current modes are observed simultaneously at the Sudbury Neutrino Observatory [9]. While the vector current interaction on the deuteron is scrupulously tested by a comprehensive set of experiments on electromagnetic observables, direct experiments on the axial-vector interaction with the two-nucleon system are scarce and have not come even close to the required precision [10, 11]. Here again, the development of EFTs during the last years has led to an important model-independent connection. It was proved that, up to the required precision in the systematic chiral expansion, these weak reactions are related by a two-nucleon current term, whose strength is parametrized by a single low-energy constant [12, 13]. The constant integrates all the short-distance physics, which is not well constrained, and is considered the main theoretical uncertainty in these processes. For the foreseeable future, the proposed MuSun experiment is the cleanest and only way to determine this constant in the two-nucleon system with 5 times higher precision than presently available there. Once the related theory program is completed, the above mentioned astrophysical reactions, as well as other important two-nucleon reactions, will be calculated in a model independent way at the same precision as the measured muon capture reaction.

The MuSun experiment must be performed under operating conditions such that the

result leads to an unambiguous extraction of Λ_d, independent of muonic atomic physics complications. At first, this seems a daunting task, as the muon kinetics in deuterium are more complex than in hydrogen. The transition between the upper μd quartet to the lower μd hyperfine state is slow and, once a $dd\mu$ molecule is formed, nuclear dd fusion occurs at a time scale of nanoseconds (because of the process of muon-catalyzed fusion). However, our studies demonstrated that these uncertainties are reduced to a negligible level at optimized target conditions of T = 30 K and 5% liquid hydrogen density.

The MuSun technique builds heavily on the R&D, equipment investments, techniques, and analysis refinements developed for the MuCap and MuLan experiments. The main distinctive features of MuSun are demanded by physics. To achieve the required target conditions, a new high-density cryogenic ionization chamber filled with ultra-pure deuterium is being developed. It will allow us to define the muon stop, identify impurities, and observe muon-catalyzed reactions, which serve as a powerful monitor to prove that the muon kinetics is quantitatively understood. The new TPC must have very good energy resolution and full analog readout using flash ADCs. This information is critical to avoid systematic uncertainties in the muon stop definition and to detect the charged particles induced by the fusion and impurity capture processes. The 5-times higher target density of MuSun, compared to MuCap, implies that the chamber does not have internal gas gain and that drift voltages up to 100 kV are needed. Additionally, a complex cryogenic system is required.

1.2 Timeline

- **PAC approval.** The MuSun experiment was fully approved by the PSI PAC in spring 2008.

- **First Engineering Run.** An existing MuCap TPC operating at room temperature was rebuilt with several newly developed components. A gold-coated pad plane was designed with high-vacuum, cryo-compatible materials, and a Kapton-based flex cable connected the pads with the high-vacuum feedthroughs, while minimizing the capacitive load. Several new electronics and DAQ components required for the final MuSun setup were tested. The run was performed in fall 2008, and is described in Section 4.

- **Main External Funding Approved.** In fall 2008, several groups within the collaboration submitted requests to their funding agencies. The physics case was well received and funding was approved in spring 2009.

- **PhD. Students Join MuSun.** Since proposal submission, several Ph.D. students and a new postdoc joined the experiment. This was an essential step as the experienced students and postdocs in MuLan and MuCap are involved in final data analysis efforts, and we had to build up a new team. The students are Justin Philips and Luis Ibanez from Boston University, Nandita Raha from the University of Kentucky and Michael Murray from the University of Illinois. Serdar Kizigul is an Illinois postdoc who has been leading the software development. All students have started software and hardware projects (c.f. Section 5).

- **Development of the Full Cryo-TPC Setup.** The construction and test of the cryo-TPC and the associated cooling and vacuum components was led by the PNPI team. A first assembly of the whole setup at PSI was achieved in November 2009. A summary of this work is presented in Section 2.

Though the progress on the challenging hardware was excellent, the collaboration decided that the technical risk of commissioning the experiment in 2009 was too high, given the complexity of the new apparatus. We postponed our first beam test of the final set-up from the end of 2009 to spring 2010. In Section 6 we update our plans for 2010 and formulate our beam request.

2 Detector Design, Construction and Tests

2.1 Design and Construction

The overall cryo-TPC and associated cooling system is described in detail in our proposal and the main functional blocks are sketched in the conceptual design in Fig. 2. All the major components were completed, allowing assembly and first tests at PSI in 2009. Construction took place primarily at PNPI with several high tech components provided by PSI and the US collaborators, including the critical cryogenic 50 pin feedthroughs on the cold flanges, which were produced and welded in the US, and the Kapton flex cables for the readout of the TPC pads in the clean D_2 gas at 30K.

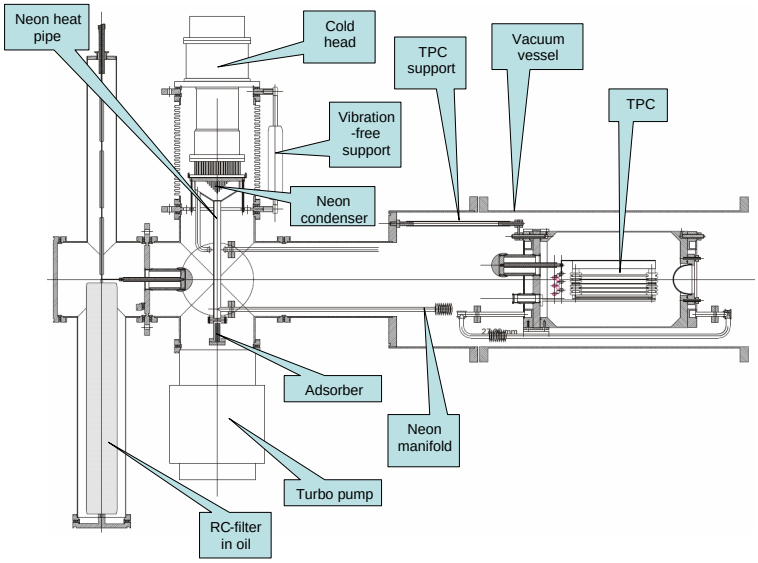

Figure 2: Conceptional design of cryo-TPC and cooling system.

The picture collection in fig 3 illustrates the progress made from the engineering design concepts towards the realization of various components. Item (1) shows the overall mechanical layout developed according to the conceptional design, while item (2) shows the fully assembled setup (with the entrance flange still open), before the first cool down at PSI. On the top of the structure is the cold head (Leybold COOLPOWER

140T). It produces the cooling power and liquefies neon in the closed loop system via a heat exchanger. The intermediate neon heat transfer system mechanically decouples the vibrations of the cold head from the sensitive TPC detector, as microphonics would deteriorate its energy resolution. Liquid neon moves by gravity through the tubes into the forward and backward heat exchangers mounted on the body of the inner pressure vessel. Item (6) presents a more detailed view. The copper ring on item (6) serves as a cooling element by liquid neon vaporization and includes a heater for temperature stabilization. Gaseous neon returns to the condenser from the top part of the heat exchangers. For the temperature stabilization we use 3 independent heaters (on the cold head and on the forward and backward heat exchangers) and 3 temperature sensors at the same positions. The figures also show the beryllium window (in dark color). Its design drawing is given in item (4). The window has been tested at room temperature up to 26 bar and at 80K up to 10 bar; at low temperatures it is tested along the saturation pressure line for deuterium, down to 32K and 5 bar. The window is attached to the chamber flange through indium sealing and has been tested over more than 35 thermo cycles (80-300K) and more than 40 pressure cycles with hydrogen and deuterium. The beryllium hemisphere (60mm diameter, 0.4 mm thickness) is welded to the stainless steel body by a thermo-diffusion method. The body of the cryo-TPC vessel was machined from one piece of aluminum alloy, electro-polished from all sides and then tested in the same way as the beryllium window. Items (3) and (5) show the CAD model of the inner part of the TPC and the first assembled TPC, respectively. One can see the pad plane, the grid, the field cage on the Macor rods (white) and the high voltage anode plane, where an α test source (Am-243) is mounted. The high voltage feedthroughs are visible in red in item (5). They will be replaced by large Ceramtec feedthroughs (see item (3)) in the final version. Several renditions for the PAD plane material were tested, the final version will be made from Macor, using a special metal plating technique.

2.2 Assembly and Performance

In November 2009, the PNPI team spent several weeks to assemble the whole cryo-TPC installation at PSI and test the performance of the combined system. Below we present the results of this work.

2.2.1 Cooling System

The cooling system was produced and installed without problems. The cooling of the chamber relies on the gravity circulation of the liquid neon in a closed loop system. Neon is cooled down in the condenser by the cold head and flows down through copper tubes (Fig. 4). It reaches the forward and backward heat exchangers on the chamber flanges through the horizontal bellows. The system is intrinsically safe, as an external volume takes up the excess, in case of emergency heating. The cooling time from room temperature in the chamber (300K) to the working temperature (30K) is 10-12 hours. An important aspect of the system is that cooling can be achieved not only with liquid neon, but cold gas as well, allowing stabilization of any temperature in the range 30-300K.

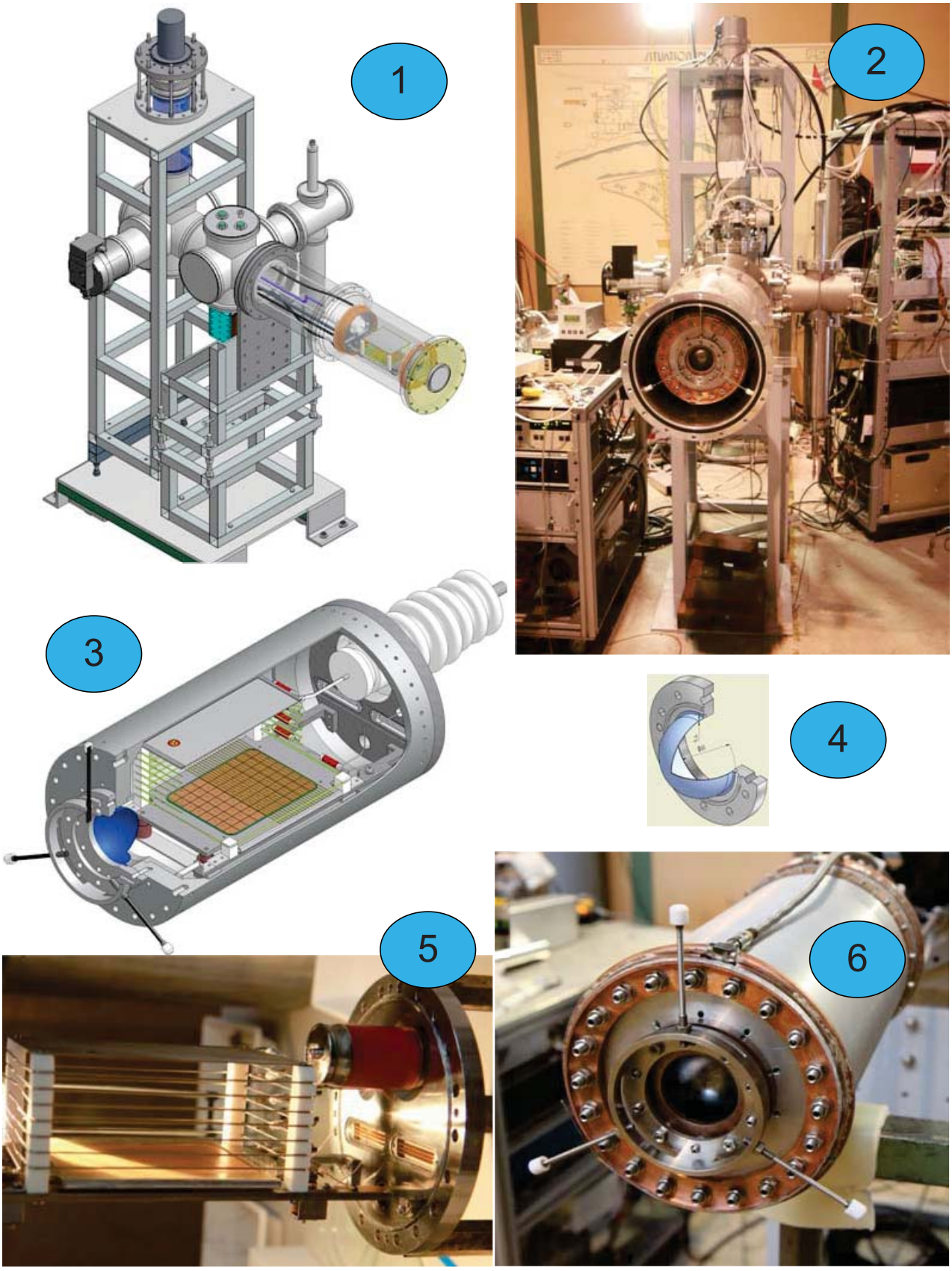

Figure 3:

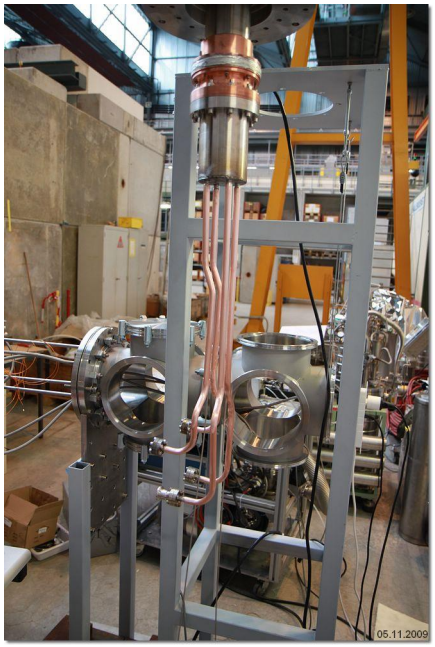

Figure 4: Vertical part of the cooling system mounted to the cold head.

The temperature was stabilized at 32 ± 0.03K (Fig. 5) and had a reserve cooling power of about 25W (electrical power supplied to the heaters to compensate the cooling). This is an excellent result, demonstrating that only 5-8W of cooling power is lost in heat transport through the vacuum and heat bridges. Possibilities for the use of the reserve cooling power include a final purification stage of the deuterium and the installation of a big cryopanel for better pumping of the system. A cryopanel can be made for water and air pumping with a pumping speed of about 2000-3000 l/s. The available cooling power would also allow the mounting and cooling of the preamplifiers close to the cold vessel, if that becomes necessary.

2.2.2 Purification (CHUPS)

The CHUPS apparatus [14] was used as a purification system for the MuSun setup. In a previous run, there were moderate problems with the vacuum insulation and a leak in the liquid nitrogen manifold was suspected. Therefore, this year the compressor unit was partly disassembled and several leaks were discovered in soldered connections near the liquid nitrogen reservoir due to the frequent temperature cycling. To prevent the leaks reappearing during the present tests, new connections were made with doubled stitch cross-section of the brazing alloy. More serious modification of this assembly is scheduled for early 2010.

A leak search in the deuterium manifolds was done after the CHUPS refilling with the leak detector in a sniffer mode. Sniffing showed few minor leaks at the level of 10^{-5} mbar·l/sec. Immediate repair of these leaks was impossible because all of them are caused by repeatedly over-tightened Swagelok couplings. The system was able to support the test run, but reassembly of the deuterium manifolds before the data taking runs is required. The next problem concerns the possible obstruction of porous stainless-steel filters installed in many places of both deuterium and nitrogen circuits.

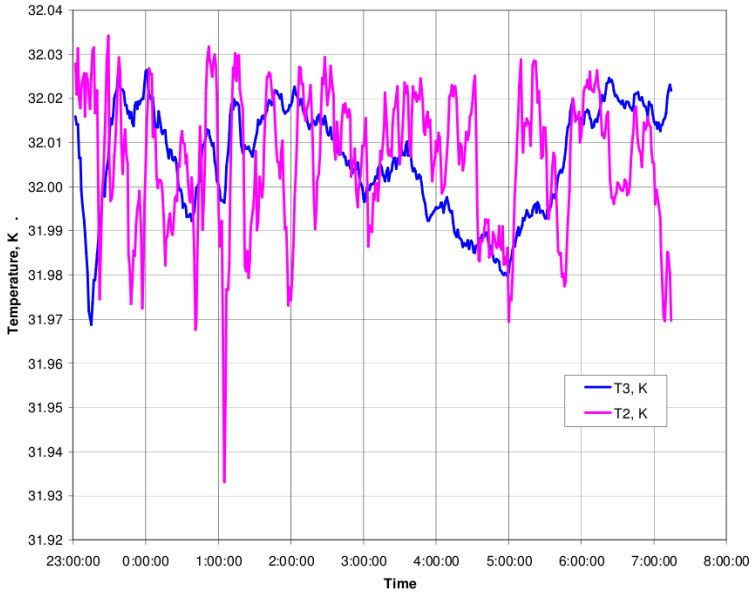

Figure 5: Temperature stabilization of the cold chamber.

The filter blocking and some additional factors lead to the relatively weak deuterium flow (in comparison with previous years). The mean value during the present tests was about 1-1.5 slpm, which is two times less than normal. The CHUPS system has been working over 5 years without problems, so it is time to perform some maintenance and refurbish the system before a production run to fulfill the very demanding purity requirements of MuSun.

2.2.3 Chromatograph

Chromatographic sampling is performed online directly from the deuterium line without sample bottles. This method allows constant clean condition of the sampling line and the capability to take more numerous sizable probes without interruption of deuterium gas flow. Measurements with online sampling appear more consistent than the older sample bottle method, and clearly this new method will save a lot of precious beam time in the future, as it does not require access to the beam area. Chromatographic data from the first and second cooling of the cryo-TPC are presented in Figure 6. One can see that during the measuring sessions the new method gave over 40 experimental points, greatly exceeding the quantity of chromatographic measurements possible with the older method. Both measurement sessions show the same behaviour for the oxygen traces: they disappear after 15-20 hours of circulation, which conforms to our MuCap experience. The best result achieved for nitrogen is less than 1 ppb, which is the new record for the purity measurements. This sub-ppb sensitivity is possible due to large probes of more than 15 liters at STP.

2.2.4 High voltage

There are two high voltage supplies: -5kV grid voltage and -100kV cathode voltage in the cryo-TPC. No problems were encountered with the -5kV system. The cathode high voltage system was mechanically assembled. It contains an external part comprised of an RC filter with the current limiting resistor in a special adapter filled with 8 liters

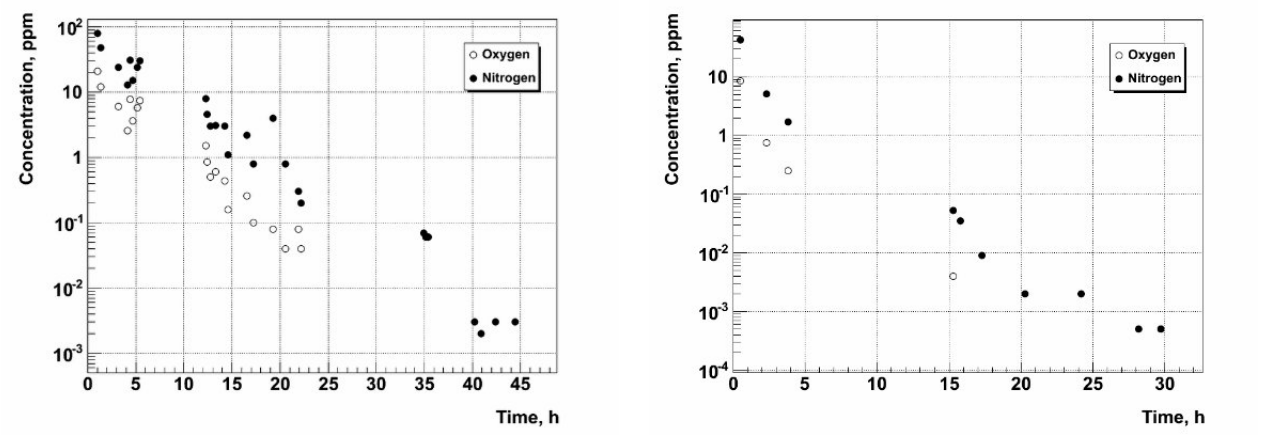

Figure 6: Impurity concentrations in the first and second cooling of the cryo-TPC.

of circuit-breaker oil. Internally, there is a high potential line made of a stainless steel tube of 6 mm diameter which connects the oil-vacuum electrical feedthrough with the vacuum-deuterium feedthrough.

The cathode high voltage was only raised to 50 kV, lower than the planned 70-100 kV operating voltage, because discharges occurred in the insulation vacuum. There are two possible locations for the high voltage breakdown. Discharges were located around the feedthrough between oil and vacuum and, while the reasons have to be investigated more carefully, we suspect that there is a poor local vacuum. There is also a known deuterium leak near the high voltage feedthrough at the cryo-TPC flange. It is a reasonable assumption that both high voltage feed-throughs have poor weld joints. In order to solve this problem, we will leak check the container of the RC filter and repair it. The deuterium leak will be sealed during the production of the new TPC flanges instead of the current test flange, which will also include the new HV feedthroughs, which already have been ordered.

The cryo-TPC was equipped with an Am-241 source with 50 Bq intensity. This alpha source is installed on the cathode plane. The alpha signals were systematically studied at various voltages at the cathode and the wire grid and showed the expected behaviour. All measurements were done at 33K and 4.5bar in the cryo-TPC.

3 Electronics Development

The new preamplifier card for the TPC, a board of 4 layers in mini-VME standard, was developed. We have four 16-channel boards at PSI and two more at PNPI. The sensitivity of the preamplifier is 100mV/MeV. The motherboard for the preamplifiers was constructed so that it fits directly onto the vacuum flange of the chamber, as shown in Fig. 7. This development was the base of a diploma project by a St. Petersburg student. The sensitivity of the preamplifiers measured at PSI was the same as measured on the lab bench. Since the noise was lower it is clear that the crate assembly provides good shielding against noise and RF. Five new amplifier boards with CAMAC form-factor were designed and produced, which provide outputs with two different dynamic ranges for the WFDs (discussed below). They will be assembled in January 2010.

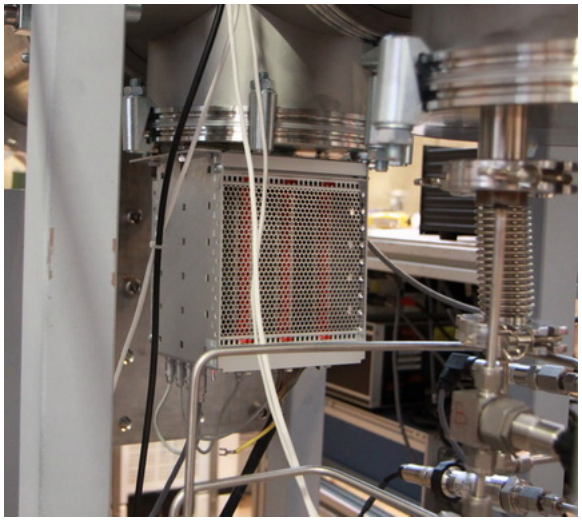

Figure 7: New low noise preamps in a crate mounted directly to the vacuum flange and 2x50 pin feedthroughts.

Shaped and amplified signals from the cryo-TPC will be read out with the 8-bit waveform digitizers (WFDs) originally developed by the Boston group for the MuLan experiment. The WFDs were designed to digitize fast pulses from photomultipliers with a 450-550 MHz sampling rate. For the digitization of slow pulses on the pads of the TPC, the firmware was modified to allow a reduction in effective sampling frequency down to 50 MHz. Like the FADCs used to read out the TPC in MuCap, WFDs continuously digitize the input, but zero-suppression logic records only intervals near pulses. This reduces the data rate from WFDs significantly compared to FADCs, making it possible to record every event without any prescaling. WFDs can run in a self-triggering mode, meaning that all pulses above a certain threshold are recorded. The most recent revision of the WFD firmware (01/2010) also permits separate *external* triggering for each of the 4 channels on the board.

The readout electronics for the MuSun electron detector will be the same as that of MuCap. The ePC, the wire chambers which form a cylinder around the TPC, will be read out, once again, with custom TDC "COMET" modules. The 64 PMT signals from the eSC, the scintillator slabs just beyond the ePC, will be read out with 500 MHz waveform digitizers (WFDs) and discriminated signals from the eSC will be read out with CAEN 767 multi-hit TDCs. CAEN TDCSs and 500 MHz WFDs will also be used to read out signals from the muon entrance counter and its associated veto counter. Neutron detectors will be read out by custom 12-bit 170 MHz FADCs.

4 Test Run with Modified MuCap TPC

4.1 Overview

The first MuSun engineering run at PSI was completed on December 18, 2008, using a proto-TPC operated at room temperature. The accumulated statistics during the run are shown in Figure 8.

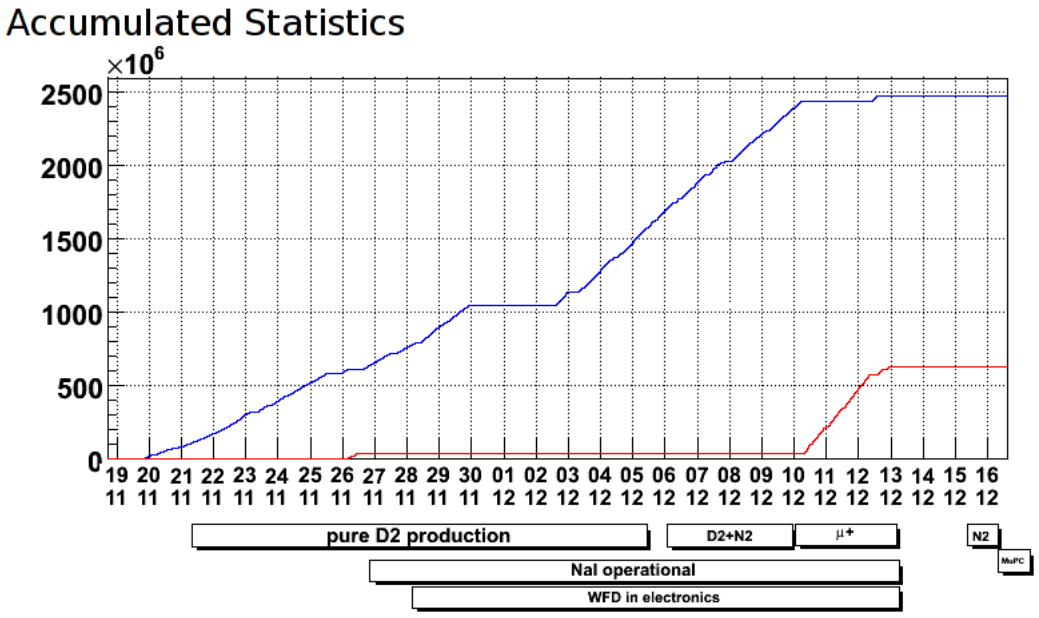

Figure 8: Accumulated statistics during the first run of MuSun. A total of $\sim 2.5 \cdot 10^9\,\mu^-$ (blue curve) and $\sim 0.6 \cdot 10^9\,\mu^+$ decays, characterized by a beam counter and subsequent electron scintillator signal, were recorded on tape.

The complete data set (∼9 TB) are now archived on the mass storage system of the National Center for Supercomputing Applications (NCSA) at the University of Illinois. An initial data quality selection has revealed that 85% of the initial data set are of good quality for further analysis. We have sorted the runs into different groups of the various experimental conditions. Among those, the two most important groups are the pure deuterium gas and periods of data taking with a nitrogen doped deuterium gas. As discussed in the proposal, the muon transfer rate from deuterium to nitrogen is not well known, but expected to be higher than for transfer from hydrogen. Moreover, nitrogen is the only impurity, which still might not be completely frozen out at the cryo conditions of the final experiment. Fig. 9 shows the significant reduction of the muon lifetime as observed in our online monitor, which fits a sample of the recorded decay spectra, when 53 ppm of N_2 was added to the previously pure D_2. Several smaller subsets have been identified for special systematic studies.

For this first engineering run, the collaboration had defined the following technical goals to be addressed with this data set:

- Develop pad readout, optimize reconstruction and resolution of the new TPC operated as an ionization chamber.
- Identify and separate fusion recoils from the muon stop, without introducing systematic distortions.
- Implement and exercise the full analog readout of the TPC in untriggered mode. This was done in steps during the run by replacing the FADC readout by the high bandwidth WFD electronics for several TPC sectors.

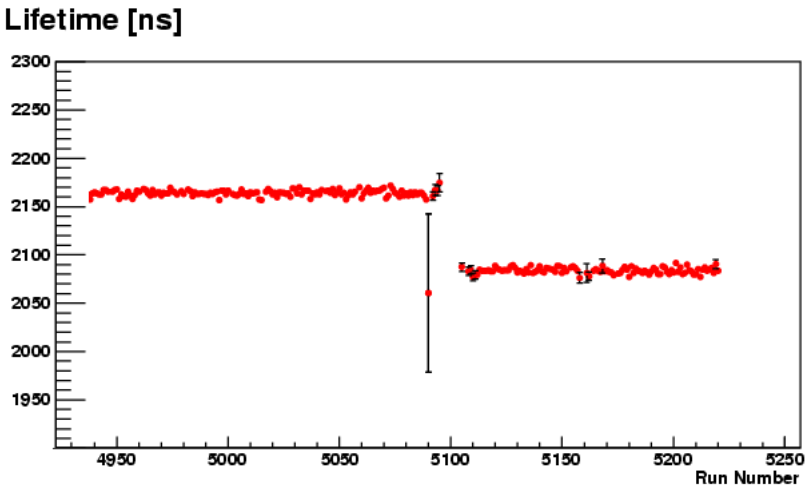

Figure 9: Online lifetime monitor of MuSun, showing significant reduction of muon lifetime after D_2 is doped with nitrogen.

These goals address some of the major issues differentiating the MuSun from the earlier MuCap experiment. The data collected in this run turned out to be extremely helpful to stimulate the development of the whole analysis chain regarding the specific features of the new pad TPC, while the final cryo-TPC was still under design and construction. In addition, the acquired data will also allow the study of the following physics goals:

- A measurement of the muon transfer rate from deuterium to nitrogen.
- The identification of high-Z impurities in the presence of the fusion background. The fusion activity after a muon stop is a another key new feature for the deuterium target compared to the protium target of MuCap.

In this section, we describe the online developments during the run, whereas the offline analysis is presented in Section 5.

4.2 Electronics and DAQ

In the engineering MuSun run, two different systems were used for the digitization and the readout of pulses on pads of TPC, the traditional MuCap system and the new system based on waveform digitizers (WFD), being the subject of R&D tests during the run.

The traditional system for TPC readout consisted of a combination of TDC400 time-to-digital converters custom built for the MuCap experiment by PSI and 12-bit flash analog-to-digital converters (FADCs). TDC400 modules record time-stamped hit patterns from TPC pads at two signal thresholds in 200 ns interval. FADCs continually digitize output from pads of TPC at 25 MHz sampling rate and record the data into internal circular buffers. The data are continually overwritten until there is an external trigger. Upon an external trigger, FADCs transfer the data from their memories to frontend computers over Ethernet cables. The 2-bit information about signal amplitudes provided by TDC400 modules is far too coarse for reliable event reconstruction.

In the offline analysis of the recorded FADC data, a most complete picture of reaction kinematics in the active volume of TPC can be obtained, including the tracks of both incoming muons and outgoing particles, their energies and associated times. FADCs provide a valuable information for R&D studies of the new TPC, for testing the experimental approach and for developing and testing the algorithms for identification of clean muon stops, separation of fusion recoils and identification of various other experimental situations. However, due to a huge data rate produced by FADCs in such a mode of operation, only a small fraction of events can be recorded. To record the events of interest, a second level trigger was implemented basing on FPGA processor, which monitors the input channels of TDC400 modules and issues a trigger for FADC if the pattern of fired pads in TPC has a valid topology. Additional triggers were generated to record greatly prescaled regular events.

The second system for TPC readout, based on the MuLan waveform digitizers (WFDs), is described above. To provide the required energy resolution and dynamic range for both low and high amplitude pulses being digitized by 8-bit WFDs, individual low and high gain outputs from each TPC pad were digitized separately. The data recorded by FADCs will be used to analyze the reliability of the WFD-based approach of event reconstruction. So far, the data analysis was concentrated on FADC data, but the methods developed for the analysis of FADC data can be naturally applied to WFD data.

The data acquisition system (DAQ) in the MuSun experiment provides the readout of frontend electronics, event building, data storage, slow control and online monitoring of the data being accumulated. MuSun utilizes a MIDAS-based DAQ inherited from its parent MuCap experiment. Minor modifications in the DAQ have been made to accommodate the new electronics and to improve the throughput for the increased data rate. In the test run, the DAQ consisted of seven major frontends and a slow control system. FADC and WFD data streams were separated from the main network into two individual subnetworks to reduce the load of the main network. The FADC subnetwork was upgraded by a managed Ethernet switch model DES-3225L from D-Link. To provide a better routing of data streams between FADC boards and network interfaces of frontend computers, the FADC subnetwork was configured into several virtual networks. For the WFD data stream, the infrastructure of the MuLan experiment was used. Two copies of data were written during the run. The master copy was written to 400MB LTO3 tapes. A backup copy was sent to the PSI archive for temporary storage. The tapes were shipped to the University of Illinois for offline analysis.

5 Analysis Framework and Projects

5.1 Development of Analysis Framework

The data analysis software is built on the existing MuCap analysis code which incorporates both MIDAS and ROOT libraries. In the first stage, raw detector signals are processed to construct more physical objects like muon and electron tracks, capture neutrons etc. While many of the basic MuCap processing modules are common to the MuSun analysis, a new muon track finding algorithm had to be developed. MuSun reads the full analog signal from the TPC for each event, whereas MuCap generally

used discriminated signals for the bulk of the data and full analog readout for a small fraction of the events. This increase in information and the difference in the topology of the TPC readout plane require a new muon identification algorithm (details are described below). The presence of charged fusion products in the deuterium environment of MuSun is another reason for necessary adaptions of the muon stop definition. Hence, the collaboration made a major effort in 2009 to develop this new algorithm. At this time, the collaboration has almost finished the development of this new code for the first stage of the analysis which will run on the supercomputer grid of NCSA at the University of Illinois. The output is stored in a standard ROOT tree format for further processing. We have also implemented an improved tree structure that is slightly more efficient with respect to the second stage of the analysis. The time spent on this development will yield a faster processing time of the output trees.

The second stage in the analysis is a very modularized framework that allows for a separate analysis of various aspects like the muon lifetime, neutron spectra, fusion recoils etc. It processes the physical objects in order to study the relevant spectra of interest (e.g. muon-electron or muon-neutron time distributions). Since this analysis step will be run several times with redefined cuts and spectra, the improvement in the processing speed mentioned above will yield a long-term profit to the collaboration.

Besides these general developments on the analysis, we also have adapted the event displays in order to study specially selected events by eye. The graphical representation of typical and very special muon tracks in the TPC and their topologies is an essential tool for developing the new muon stop definition. Throughout the MuCap analysis, we have regularly utilized the event display, and it has been crucial for defining and verifying the analysis algorithms.

5.2 TPC analysis

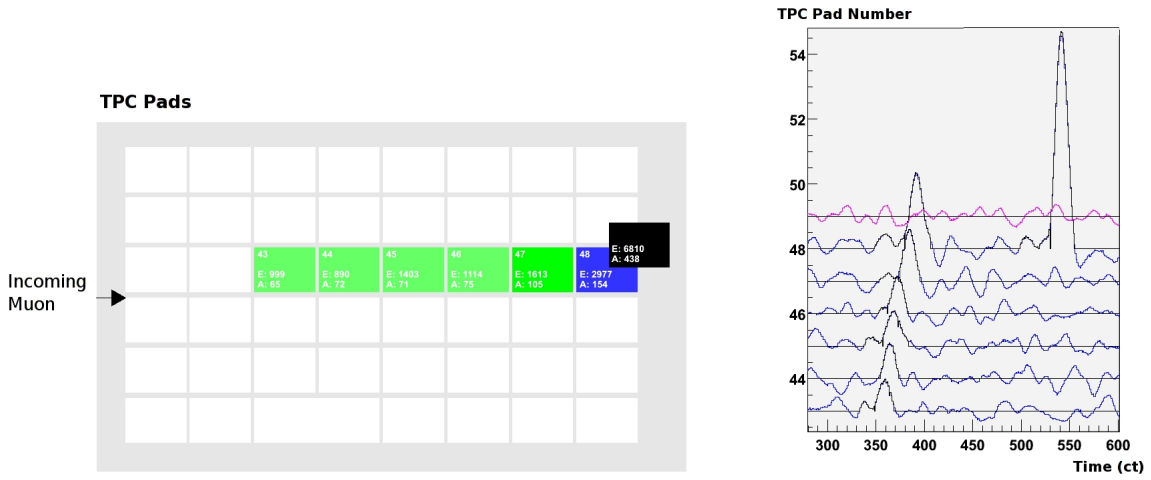

(a) (b)

Figure 10: A sample muon entrance is depicted with (a) the event display with the TPC pad structure and (b) the representation of the analog readout.

The proto-TPC consists of 80 pads and collects energy deposition signals from muons and from the charged fusion products (proton, ^{3}He and triton). An event display module

was developed to show TPC events. On the TPC pad plane, each identified pulse is plotted and color-coded depending on the fitted energy. An example of a muon track with a fusion pulse is given in Figure 10(a). Green colors are selected for the energy range corresponding to the main muon track, with darker greens representing higher energies. Blue colors designate higher energy pulses, including energies corresponding to the Bragg peak of the muon stop. The black colored box indicates an even higher energy pulse, most likely a fusion event. In this display, the fusion pulse occurs on the same pad as the stop, and is depicted as an additional box that is slightly displaced.

The event display also shows pulses as they are originally recorded in the FADCs. Figure 10(b) represents the FADC analog samples for the same event. Only those pads that have pulses exceeding the noise are drawn in blue. The magenta colored line indicates that the pad is adjacent to the muon stop pad. The black lines drawn underneath the raw pulses represent samples that are identified by the pulse finder as part of a pulse. Both types of event displays are available for each event.

5.2.1 Pulse Finder

The pulse finder algorithm has been developed specifically to catch small muon track pulses in the FADC data. The pulse finding starts with pedestal fitting and subtraction. The 1024 samples within one recorded FADC event are projected onto the energy axis, as in Figure 11. Since the number of FADC samples is large compared to the width of a typical muon pulse, the dominant feature of the projection is a gaussian distribution of the pedestal allowing for the extraction of the pedestal energy and sigma. The pedestal offset is then subtracted from FADC counts, and the pulse finder searches for the pulses. Any three consecutive bins with a value larger than 4 pedestal sigma are considered as a pulse seed. Once the pulse seed is determined, positive samples to the left and the right of the seed are accepted as a part of the pulse.

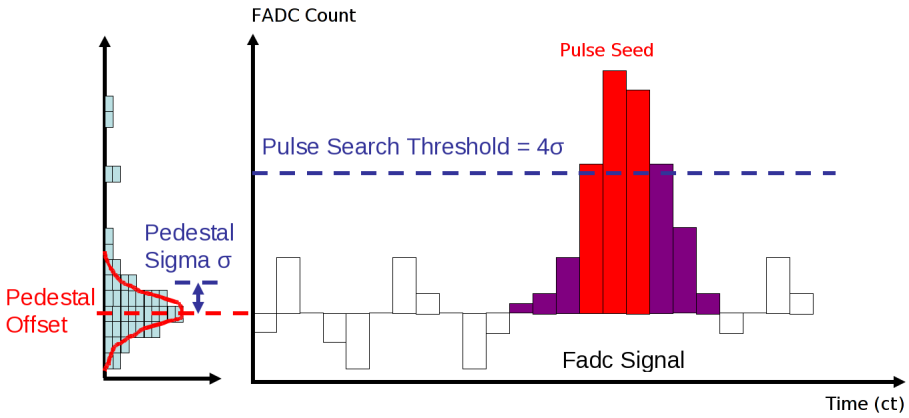

Figure 11: FADC pulse finder. Details are described in the text.

Identified pulses are sorted in time, attached to the nearest muon entrance signal and then the pulse characterizing parameters (e.g. time, amplitude, area etc) are saved into a tree.

5.2.2 Muon Track Finder

The goal of the track finder software is to use the reconstructed pulses in order to determine the muon trajectory and its stop location as well as to identify subsequent fusion products. For this we have developed a novel track finding algorithm. To improve the overall tracking reconstruction, we have first calibrated all pads to have similar gain by using the monoenergetic ^{3}He fusion signals.

Figure 12 depicts a typical event and outlines the main features of the track finder. In a first step, the first pulse above a certain amplitude threshold is considered as a possible track seed. We then search in a continuously adapted cone in both the forward and backwards region of this seed with respect to the beam axis. The pads in Fig. 12 surrounded by a colored box are identified as a possible muon track in this event and clustered together. This algorithm continues until no further track seed can be found. In the given examples, there are a few pads with light green color that do not qualify as a seed since their pulses are too small. The muon stop pad also has a possible subsequent fusion pulse that is stored separately. The clustered pads are then stored in the output tree for further analysis.

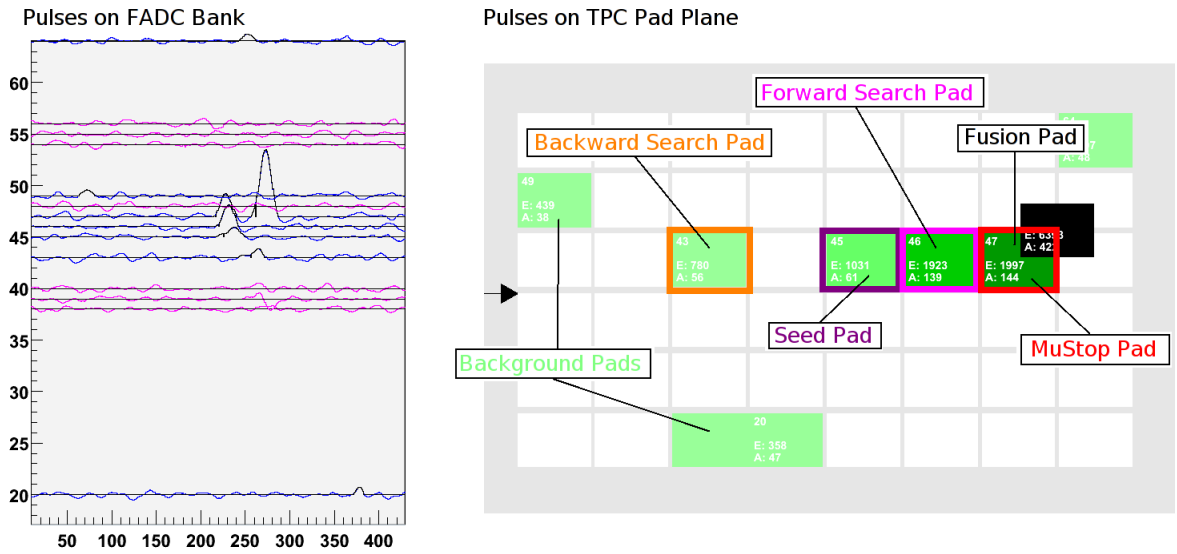

Figure 12: TPC track finder example. Details are given in the text.

Having this muon track identification, we have started to study the resolution of the TPC using the monoenergetic ^{3}He pulses. Here, we selected good muon stops in the TPC with a delayed fusion signal. The ^{3}He pulse energy distribution from a small subset of the data is given in Figure 13. The gaussian fit shows the energy resolution of the ^{3}He pulses is about 10 percent equivalent to $\sim$80 keV. However, the final determination of the chamber resolution needs more careful work which is currently in progress.

5.3 Electron Analysis

The electron analysis for MuSun will follow very closely that of MuCap. For the final configuration, an electron object will consist of a track in the ePC accompanied by a 4-fold coincidence in the eSC, the scintillator barrel which surrounds the MuSun detector

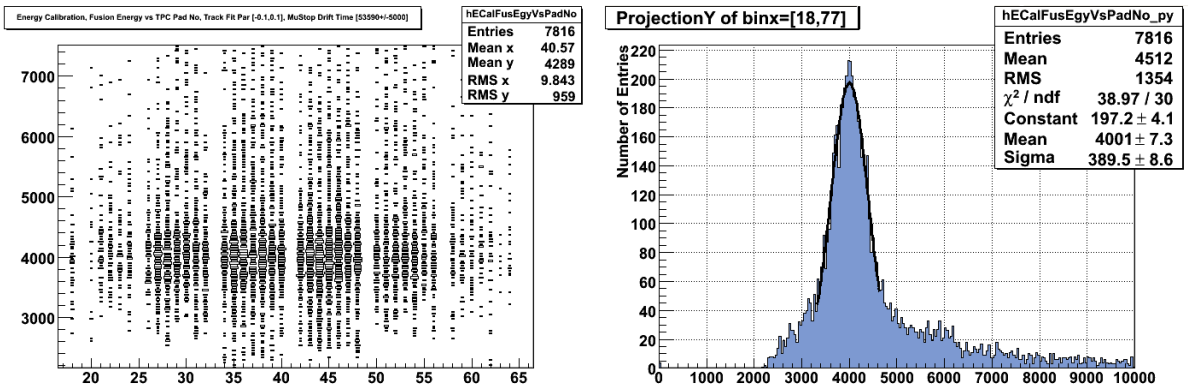

Figure 13: ^{3}He fusion pulse energy distribution. Left panel: Fusion pulse area versus pad number for the center region of the TPC. Right panel: Sum of all fusion pulses for all pads with a gaussian fit.

(two layers of scintillator, each of which is read out at both ends). However, in this first run, the wire chambers which comprise the ePC had been removed for repair and only the eSC signals were available.

The WFD signals from the eSC look much as they did for the MuCap runs. The typical pulse height is only about 1/6th of full scale while the pulse height for the muon entrance counter (see figure 14 lhs) is much larger. The time associated with each pulse consists of an *island time*, which gives the time of the first in a set of samples, plus a small offset. The latter is computed several different ways: the time of the maximum value, a mean time derived from an arithmetic average of the 7 samples around the peak and a constant fraction time, an estimate of when the pulse reaches 50% of its maximum value, above pedestal. We demonstrated in the MuCap analysis that there was no compelling reason to choose one over any of the others. The main analysis

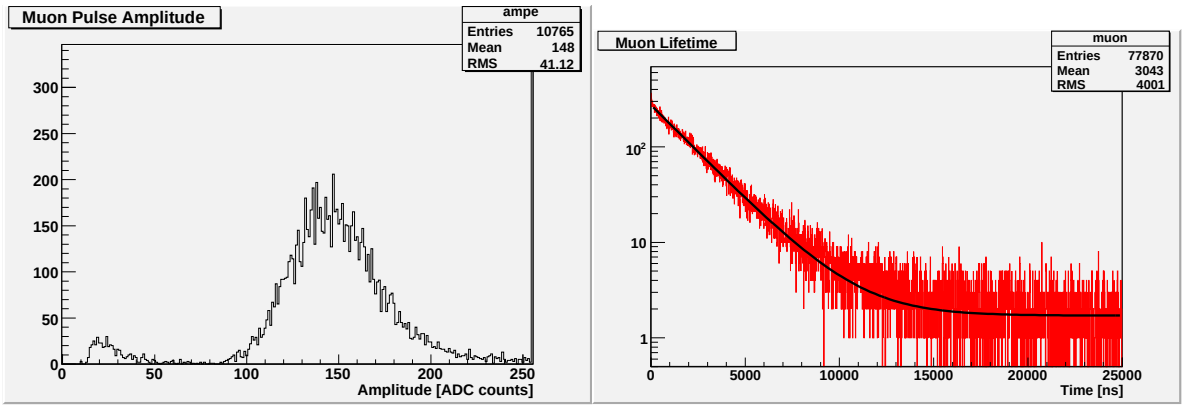

Figure 14: Electron analysis with new framework. lhs: Pulse Height Spectrum for Muon Entrance Counter. rhs: Sample Muon Lifetime Spectrum.

challenge consists of understanding fits to the muon decay spectra, the time between a muon stop and the appearance of a decay electron. However as a proof of principle,

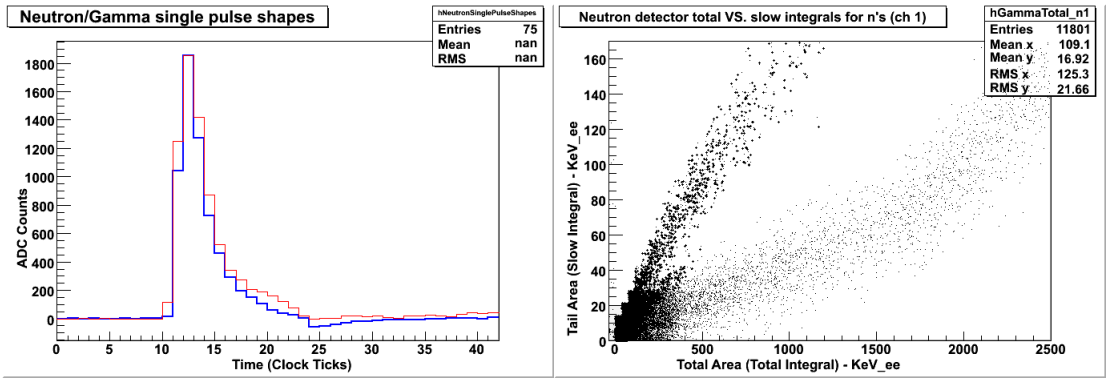

Figure 15: Neutron/gamma discrimination in liquid scintillator. lhs: typical pulse shapes recorded by 12-bit, 170 MHz waveform digitizers. The red neutron pulse has a slightly longer slow component compared to the blue gamma-ray pulse. rhs: Full pulse amplitude (horizontal axis) versus pulse tail amplitude (vertical axis). Lower band corresponds to gamma-rays, while upper band corresponds to neutrons. Energy axis given in equivalent electron energy MeV_{ee}.

while the muon stop analysis is still under development, Boston University graduate student Luis Ibanez has used the time of a muon arrival in the entrance scintillator as our start signal. The decay lifetime derived from the spectrum, shown in the right panel of Fig. 14, is consistent with expectations. His next task will be the determination of the important μd to μN transfer rate. This rate is not well known but was measured in the 2008 engineering run.

5.4 Neutron Analysis

Muons in deuterium yield two distinct sources of neutrons: (i) fusion neutrons following $d\mu d$ molecule formation and the subsequent $dd \rightarrow {}^3He + n$ fusion reaction, and (ii) capture neutrons following the $\mu^- d \rightarrow nn\nu$ capture reaction from the muonic deuterium $F = 1/2, 3/2$ hyperfine states. The $d\mu d$ fusion neutrons are monoenergetic with energies of 2.45 MeV. The pair of coincident neutrons from μ^-d capture – although peaked at energies 1.3 MeV – include an energetic component that extends to 53 MeV.

Encoded in this time dependence of the fusion neutrons are the $dd\mu$ molecular formation rates from the $F = 1/2, 3/2$ hyperfine states (Λ_{dd}^Q and Λ_{dd}^D) and the hyperfine transition rate between the two hyperfine states (Λ_{qd}). Consequently, the detection of fusion neutrons should enable the determination of the kinetics parameters Λ_{qd}, Λ_{dd}^Q and Λ_{dd}^S that are important in the extraction of the μ^-d doublet capture rate Λ_D from the decay electron time spectrum. The detection of μ^-d capture neutrons is more challenging but also offers a method of determining both the hyperfine transition rate Λ_{qd} and the hyperfine capture ratio Λ^Q/Λ^D.

In our Fall 2008 engineering run we used two newly constructed neutron detectors that viewed the prototype time projection chamber. Both neutron counters were cylindrical cells containing 1.1 liters of EJ-301 organic scintillators (detector one) or EJ-309 organic scintillator (detector two) and coupled to 13 cm diameter photomultipliers. The neutron counters were read out by two channels of 12-bit, 170 MHz custom-built wave-

form digitizers. Goals of the neutron studies for the 2008 run include: the development of the neutron analysis framework for the MuSun experiment, the identification of the 2.45 MeV neutrons from the $d\mu d$ fusion reaction, and various studies of signal rates, background rates, instrumental resolutions, *etc.*

Kentucky graduate student Nandita Raha is analyzing the neutron dataset to obtain the time spectra between muon stops in the deuterium gas and neutron signals from $d\mu d$ fusion and μd capture in the liquid scintillators. Cuts must be applied to both identify the μ^- stops in D_2 gas and separate the neutron signals from background sources. The background sources include both gamma-rays originating from electron bremsstrahlung following muon decay and neutrons originating from $Z > 1$ nuclear muon capture, photo-nuclear reactions, accelerator sources and cosmic-rays. As an example of the ongoing analysis work on the 2008 neutron dataset we show in Fig. 15 the neutron/gamma pulse-shape discrimination. It is based on the relative amplitudes of the slow components of the scintillation light arising from the gamma-ray signals and the neutron signals in the liquid scintillator and is is derived from the ratio between the amplitudes of the full pulse and the pulse tail that was recorded in the 170 MHz waveform digitizers. The left panel shows a sample neutron pulse and gamma pulse superimposed. In the right panel, the distribution of full pulse amplitudes to pulse tail amplitudes is plotted, which shows separate bands from neutron signals and gamma-ray signals.

5.5 Monte Carlo Simulation

The studies for the proposal were made with a GEANT3 model, based on the MuCap experiment. As Monte Carlo studies of systematic effects will play an important role for the MuSun experiment, we have now developed a new GEANT4 based model, which provides a flexible framework for the envisioned physics and geometry upgrades. Special emphasis is placed on a highly flexible output structure, which can be adapted to the physics challenges we encounter during the experiment.

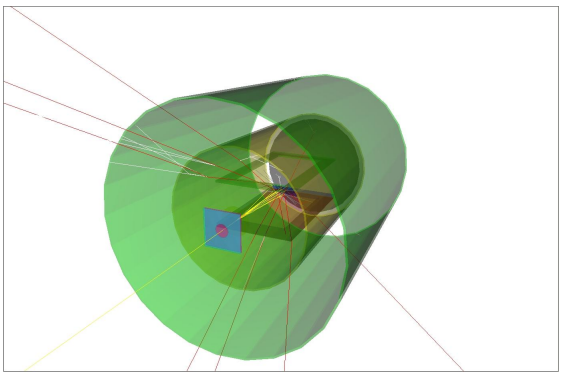

Figure 16: Simulated muon decay events.

The MuSun model is being constructed to simulate events based on a measured distribution of incoming negative muons with stopping distributions in a TPC chamber of deuterium gas. Sensitive detectors are attached to appropriate volumes, such as the muon entrance counters, anode pads within the TPC, and electron wire chambers

to mimic the data read out in the experiment. The output of the simulation is then reprocessed into the "proper" data structure and folded with the detector response functions, to simulate the experimental data stream.

In the near future, we intend to implement custom processes that are not currently in the GEANT source code. Improved definitions of muon capture and muon catalyzed fusion are top priorities to code into the simulated physics. Dedicated high statistics runs are planned for a careful study of the interference between muon tracks and fusion events, to test that the tracking algorithm does not introduce subtle time distortions. While many detectors only require a few basic variables for output (for example, simply time and energy deposition for scintillators), attaching sensitive detectors that read out much more (such as 4-momentum or the creation process of a particle) will soon be possible. These should be well-suited for smaller runs to address unforeseen systematic studies. The geometric model also needs to be completed based on the final cryo-TPC geometry. Boston graduate student Justin Phillips has taken over the development of the MuSun Monte Carlo.

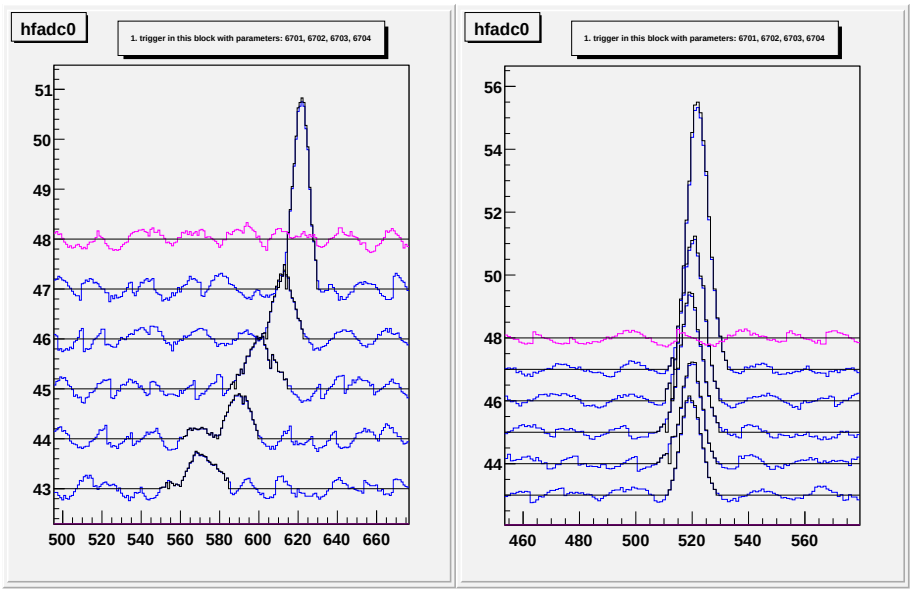

Figure 17: Simulated muons stop signals for gas density 1% (lhs) and 5% (rhs) of liquid deuterium density.

Figure 16 shows 10 simulated muon decay events illustrating the current volumes in the GEANT model. Yellow tracks are incoming negative muons, which first pass through the muon entrance counters (blue and red). They then stop in the TPC, where the energy deposition and position is recorded in the fiducial volume. Electrons are shown as red tracks, which go through the TPC walls and pass (optimally) through the ePC wire chambers (both green), recording the appropriate information. Neutrinos (gray tracks) are killed immediately after muon decay. Sensitive detectors attached to volumes visible in the above graphics (muon entrance scintillators, TPC fiducial volume, electron wire chambers) and those that are not visible (muon entrance wire chamber, electron scintillators) give output that reconstructs to all observable data.

Fig.17 shows the pad signals for a typical muon stop for the test run and the ex-

pected cryo-TPC configuration. The Monte Carlo generated pulses were folded with the realistic electronic noise spectrum as observed during the test run. As the cyro-TPC will be operating with 5-times higher density, the charge deposition is increased and the muon signal is better separated from noise.

6 Plans and Beam Time Request 2010

2010 will be an important and exciting year for the MuSun experiment. We want to finish various preparations in early 2010 and then commission the detector with muon beam during a short beam time following the PSI accelerator shut-down. Based on the experience gained during commissioning, we will fine-tune the hardware, analyze the detector performance achieved, and perform final upgrades if necessary. To complete this work, several months during summer and early fall are required. Thus we ask for our main beam time to be scheduled at the end of 2010. This will be the first MuSun production run over a 7 weeks period. In the following brief sections, we outline the collaboration's work plan and summarize our beam request.

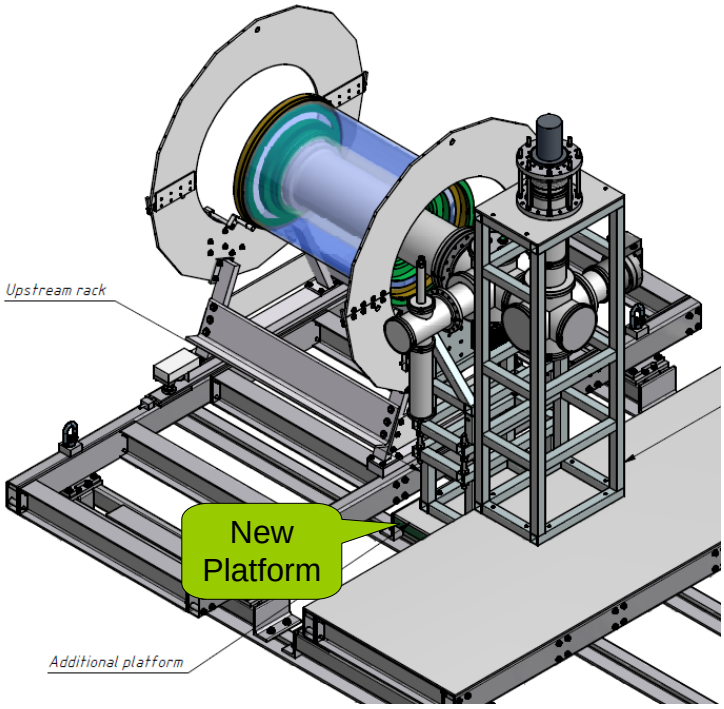

Figure 18: Design draft of MuSun support system on rails.

6.1 Collaboration Plans and Tasks

- **Repair and assembly of MuSun electron wire chamber system**. After the last MuCap run, the cylindrical wire chamber system consisting of ePC1 and ePC2 had to be removed from the electron tracker to repair a broken wire in the outer larger chamber. This repair has been done by the PSI detector group. In February/March 2010 members of the Illinois group will reinstall the chamber system. This is a labor intensive task, as the whole frame mounted

preamplifier system has to be reinstalled, the noise performance tuned and the complete chamber system trained back to high voltage operation.

- **New support rail system.** A new support system for the cryo-TPC will be built at PSI and integrated with the existing MuCap area rail system as sketched in figure 18.

- **Cryo-TPC system**. Mid March the PNPI team will arrive. In April they will be joined by the full collaboration for the integration of the new cryo-TPC system into the DAQ electronics and the other detector systems. The task list includes:

  March
  Installation of new elements of the high voltage system.
  Vacuum and cryogenic tests with the new HV elements.
  Installation of new grid and Macor pad plane into cryo-TPC.
  Installation of new Kapton flat cables.
  Repairing of CHUPS.
  Assembling of new cryogenic Impurities Concentration System (ICS).
  Measurement of the isotopic purity of the deuterium at ETH Zürich.
  April
  Common tests of the system. (Cryogenic, vacuum, slow control).
  Suppression of the mechanical resonances at cryogenic temperatures.
  Optimization of the TPC resolution based on signals from an α-source.
  Calibration of the temperature sensors in cryo-TPC.
  Connecting of cryo-TPC to circulation system (CHUPS) and ICS purification.
  Test of the ICS and impurity detection at the 1 ppb level.

- **DAQ and electronics.** The MuSun DAQ must provide stable data taking over a prolonged period of time, handle a high (15 MB/s) data rate and must not introduce any significant dead times. In March/April, we are planning to upgrade the outdated backend computer with a much more powerful PC. The DAQ infrastructure of the MuLan experiment will be incorporated into the readout, compression, and storage of data. This includes dual-processor frontend computers, a gigabit network and a set of computers for semi-offline analysis of the data. The technical run in spring 2010 will be a good opportunity for benchmarking the complete system. The time between the technical run and the production run will be used to fix all possible problems/bottlenecks should any be discovered. We are planning to upgrade FADCs that read out the neutron detectors with a faster and more powerful FPGA model. The sampling rate will be increased from 170 MHz to 250 MHz. The amplifiers reading out the TPC will be replaced with new custom built modules. The new amplifiers feature both low gain and high gain outputs to be connected directly to WFD boards. The new WFD firmware will allow the use of external discriminators with slower shaping time than the recorded waveforms. The TDC400 modules will be completely eliminated, requiring an update of the master logic firmware.

- **Detector integration**. In early May, we plan to integrate the new cryo-TPC system with the refurbished and upgraded electron detector, neutron, and beam counter systems in the experimental area.

6.2 Beam Time Request

Our beamtime request for 2010 is a follows:

- **3 weeks in May 2010 in the area $\pi E3$ immediately following the winter shutdown, once stable beam conditions have been re-established. Preferentially the standard MuCap beamline including MuLan kicker should be installed.**
- **7 weeks of beam time + 1 week setup from November to December 2010 in the area $\pi E3$ at the end of the running period. For this first production run it is mandatory that the standard MuCap beamline including MuLan kicker is installed.**
- **1 week of test beam in $\pi E1$ at a suitable transition time between experiments, to investigate the feasibility of running in this area after 2011.**

The last request addresses our concern regarding the phasing out of nuclear/particle physics experiments in the $\pi E3$ area by 2012. Though the collaboration is working at a fast pace and as hard as it can, MuSun is a complex, precision experiment still under construction and it is very likely that data taking beyond 2011 is needed. During our intense preparation efforts, we have not encountered problems that would jeopardize the precision anticipated for the experimental goal, the $\mu + d$ capture rate. MuSun will be by far the best measurement of a weak process in the two nucleon system, with high impact on modern effective field theories and basic astrophysics reactions. We gratefully acknowledge the support expressed by Prof. Joel Mesot and the PSI management to find a solution to this scheduling problem and are committed to working closely with PSI to find an alternative which will allow MuSun to reach its full physics potential.

References

[1] MuSun Collaboration (http://www.npl.uiuc.edu/exp/musun):
V.A. Andreev, R.M. Carey, V.A. Ganzha, A. Gardestig, T. Gorringe, F.E. Gray, D.W. Hertzog, M. Hildebrandt, L. Ibanez, P. Kammel, B. Kiburg, S.A. Kizilgul, S. Knaack, P.A. Kravtsov, A.G. Krivshich, K. Kubodera, B. Lauss, M. Levchenko, K.R. Lynch, E.M. Maev, O.E. Maev, F. Mulhauser, M. Murray, F. Myhrer, C. Petitjean, G.E. Petrov, J. Phillips, R. Prieels, N. Raha, G.N. Schapkin, N. Schroeder, G.G. Semenchuk, M.A. Soroka, V. Tishchenko, A.A. Vasilyev, A.A. Vorobyov, N. Voropaev, M.E. Vznuzdaev, P. Winter.

[2] Andreev, V. A. et al. *Phys. Rev. Lett.* **99**, 032002 (2007).

[3] Weinberg, S. Phys. Lett. B, **251**, 288 (1990); Nucl. Phys. B, **363**, 3 (1991); Phys. Lett. B, **295**, 114 (1992).

[4] Ando, S., Park, T. S., Kubodera, K., and Myhrer, F. *Phys. Lett.* **B533**, 25–36 (2002).

[5] Chen, J.-W., Inoue, T., Ji, X.-d., and Li, Y.-c. *Phys. Rev.* **C72**, 061001 (2005).

[6] K. Kubodera and F. Myhrer; E. Epelbaum and Ulf-G. Meissner, private communication.

[7] Bardin, G. et al. *Nucl. Phys.* **A453**, 591 (1986).

[8] Cargnelli, M. et al. In *Proceedings of the XXIII Yamada Conf. on Nuclear Weak Processes and Nuclear Structure, Osaka, Japan*, (1989).

[9] Aharmim, B. et al. *Phys. Rev. Lett.* **101**, 111301 (2008).

[10] Butler, M., Chen, J.-W., and Vogel, P. *Phys. Lett.* **B549**, 26–31 (2002).

[11] Chen, J.-W., Heeger, K. M., and Robertson, R. G. H. *Phys. Rev.* **C67**, 025801 (2003).

[12] Park, T. S. et al. *Phys. Rev.* **C67**, 055206 (2003).

[13] Butler, M., Chen, J.-W., and Kong, X. *Phys. Rev.* **C63**, 035501 (2001).

[14] Ganzha, V. A. et al. *Nucl. Instrum. Meth.* **A578**, 485–497 (2007).